*Elastomer*
Vol. 39, No. 2, pp 142~152 (2004)

# Characterization of Crazing Behavior in Polystyrene

Dae Jin Jeon, Seok-Ho Kim, and Wan-Young Kim*
*Kumho Tire Co., R&D Center, Gwangsan-gu, Gwangju, 506-711, Korea*
**Dept. of Chemical Engineering, Chonbuk National University, Chonju, 561-756, Korea*
(Received May 1, 2004, Revised and Accepted May 20, 2004)

# Polystyrene 의 Crazing 거동 특성

전 대 진† · 김 석 호 · 김 완 영*
금호타이어 기술연구소 · *전북대학교 화학공학과
(2004년 5월 1일 접수, 2004년 5월 20일 수정 및 채택)

**ABSTRACT** : Tensile tests of two types of injection-molded polystyrene(PS) samples have been carried out over a wide range of temperature and strain rates in order to characterize their crazing behaviors. Mechanical properties were affected by the formation of crazes as well as test variables. Below the brittle-ductile transition temperature, the tensile stress and the ultimate elongation increased with the molecular weight, strain rate, and with decreasing temperature while the number and average length of crazes also increase. The crazing stress increased with molecular weight, strain rate, and with decreasing temperature. However, the dependence was small compared to the tensile stress. The gap between crazing stress and tensile stress which represents time for craze formation and growth increased with molecular weight, strain rate, and with decreasing temperature. Crazing was activated near the $\beta$-relaxation temperature; crazing stress abruptly decreased at this temperature. During the tensile test, the craze density changed exponentially with the applied stress. At the initial stage, crazes formed slowly. Once a certain number of craze formed, however, the craze density increased rapidly. Craze nucleation and growth occur simultaneously.

요 약 : 서로 다른 두 종류의 폴리스타일렌(PS)을 injection 기계를 이용하여 인장 시편을 만들고, 온도와 인장 속도에 따른 crazing 거동 특성을 연구하기 위하여 다양한 시험을 하였다. 기계적 물성은 craze 형성 뿐만 아니라 다양한 시험 변수에 의해 영향을 받으며, brittle-ductile transition 이하의 온도에서의 인장 응력 및 최대 신율은 분자량, 인장 속도의 증가 및 온도의 감소에 따라 증가하며 craze의 수와 평균 길이 또한 증가한다. Crazing 응력도 동일한 형태로 증가 함을 보여 준다. 그러나, 이러한 특성은 인장 강도에 미치는 영향과 비교했을 때 보다 의존도는 상대적으로 낮다. Craze 형성과 성장에 필요한 시간으로 설명할 수 있는 crazing 응력과 인장 응력간의 차이는 분자량, 인장 속도에 따라 비례적으로 그리고, 온도가 감소함에 따라 증가 함을 보여 준다. Crazing 은 $\beta$-relaxation 온도 근처에서 활성화된다. 이 온도에서는 crazing 응력이 급격하게 감소함을 나타낸다. 인장 평가시 craze 밀도가 적용된 응력에 따라 기하 급수적으로 증가되는데, 개시 단계에서는 craze는 서서히 형성되며, 일단 일정한 수만큼의 craze가 형성이 되면 craze 밀도가 급속도로 증가했다.

*Keywords : crazing behavior, polystyrene*

† 대표저자(*e-mail : djjeon@tire.kumho.co.kr*)

# Ⅰ. Introduction

Craze formation is considered as an important mode of plastic deformation in amorphous glassy polymers and a precursor to crack propagation. Crazes form under stress, and/or in the presence of an active environment, influence the mechanical and optical properties, and permeability. Crazes act as the principal source of energy dissipation[1,2] and thus raise the toughness of thermoplastics. True cracks result from that breakdown of the fibrils leads to large voids which ultimately results in the formation of true cracks.[3,4]

Several investigations[5-8] have been already carried out in amorphous polymers, to relate the features of the fractures surface to craze and fracture mechanisms. In these studies, the fractography has been analyzed by using various techniques such as optical microscope, scanning electron microscope, and by examination of surface replicas. However, an in-depth study concerning the effect of strain rate and temperature on crazing is lacking in the available literature.

The main objective of the present research is to fill thus gap of knowledge mensioned above by understanding the basic mechanisms of the crazing process and behavior of injection-molded polystyrene (PS) samples of varying molecular weight. Emphasis is given to various other parameters also such as temperature and strain rate.

# Ⅱ. Experiment

## 1. Materials and Characterization Methods

The materials used in this research were PS homopolymers which are EA 3000 (MF 1.8) and MC 3700 (MF 19) obtained from Chevron Chemical Company. A waters 150 gel permeation chromatogram (GPC) with polystyrene gel packed column was used to determine the molecular weight and the molecular weight distribution. For calibration of GPC, a series of known molecular weight standards were used. A solution of 0.025% PS in THF was injected into the column with a flow rate of 1.0 ml/min. A Du Pont 990 thermal analyzer was used to determine the glass transition temperature(Tg). A sample weight of 4-6 mg was used and at a heating rate of 10 ℃/min from 40 to 200 ℃. Dynamic mechanical thermal analyzer (DMTA) measurements were carried out to determine the dynamic mechanical properties in the temperature range of -50 to 130 ℃, at heating rate of 1 ℃/min. A bending mode was used for the test with a frequency of 1 Hz and an amplitude of 64 $\mu$m.

## 2. Tensile Testing

Tensile specimens were prepared with a injection molding machine (Boy 15S), using an injection molding ASTM D638 type I dumbbell mold. The conditions used for injection molding are shown in Table 1. Stress-strain tests were carried out using an Instron tensile testing machine equipped with an environmental chamber. Tests were performed at different strain rates (0.005 to 1.270 $min^{-1}$) and at different temperatures (-20 to 100 ℃). Specimens were mounted on mechanical clamps 10 cm apart and allowed to reach an equilibrium temperature for 15 minutes before testing. After reaching equilibrium, the crosshead was adjusted to give zero tension. In order to assure equilibrium at each test temperature, a thermocouple embedded into another specimen was mounted inside the chamber. The

**Table 1. Injection Molding Conditions for Preparing the Specimens**

| Materials | Die Zone Temp., ℃ | |
|---|---|---|
| EA-3000(MF1.8)<br>MC-3700(MF19) | 232<br>227 | |
| Cycle Time, sec | Injection Forward<br>Feed<br>Mold Closed<br>Mold Open | 10<br>5<br>20<br>10 |
| Pressure, psi | Injection Pressure<br>Back Pressure | 2000<br>250 |

temperature inside the chamber was controlled within accuracy of 1 ℃. During the tensile tests, crazing onset stress for each test conditions was determined visually and recorded with the aid of a marker. A small lamp was mounted behind the specimen to clearly visualize the forming crazes. Three specimens were used to obtain stress- strain behavior. The normal strain rate was calculated as the crosshead speed divided by initial length of the specimen between clamps and has the unit of ($min^{-1}$). The change in craze density of both MF1.8 and MF19 at room temperature were determined at a strain rate of 0.127 $min^{-1}$ . In this experiment, specimens were randomly collected from the range of crazing onset to fracture during straining. The number of crazes and the average length of crazes in the whole specimen area were determined by using an optical microscope and cathetometer.

The structure of crazes in a bulk specimen was examined by using an atomic force microscope (AFM). For this experiment, pre-crazed tensile specimen of MF1.8 tested at 40 ℃ and a strain rate of 0.013 $min^{-1}$ was prepared and conditioned in the air at room temperature for 48 hours. Then, the specimen was cut to a dimension of 2 x 2 x 5 $mm^3$ and the surface was microtomed until crazes inside the specimen were reached.

## Ⅲ. Results and Discussion

### 1. Raw Material Characterization

The number and weight average molecular weight and polydispersity index values of PS obtained from GPC are shown in Table 2. MF 19 shows broad molecular weight distribution than MF 1.8. The commercial PS used in this experiment showed broad molecular weight distribution. The glass transition temperature ($T_g$) measured by DSC and DMTA are shown in Table 3 and Figure 1. A lower Tg results from decrease in molecular weight due to increase of chain end concentration and mobility. Tg obtained from DMTA showed higher values than

**Table 2. Number and Weight Average Molecular Weight and Polydispersity Index**

| Type | MF1.8 | MF19 |
|---|---|---|
| Grade | EA3000 | MC3700 |
| $M_n \times 10^{-4}$, g/mole | 12.5 | 5.8 |
| $M_w \times 10^{-4}$, g/mole | 36.4 | 26.6 |
| $M_w / M_n$ | 2.90 | 4.58 |

**Table 3. Glass Transition Temperature from DSC and DMTA**

| Items | MF1.8 | MF19 |
|---|---|---|
| DSC, ℃ | 104 | 93 |
| DMTA, ℃ | 110 | 93 |

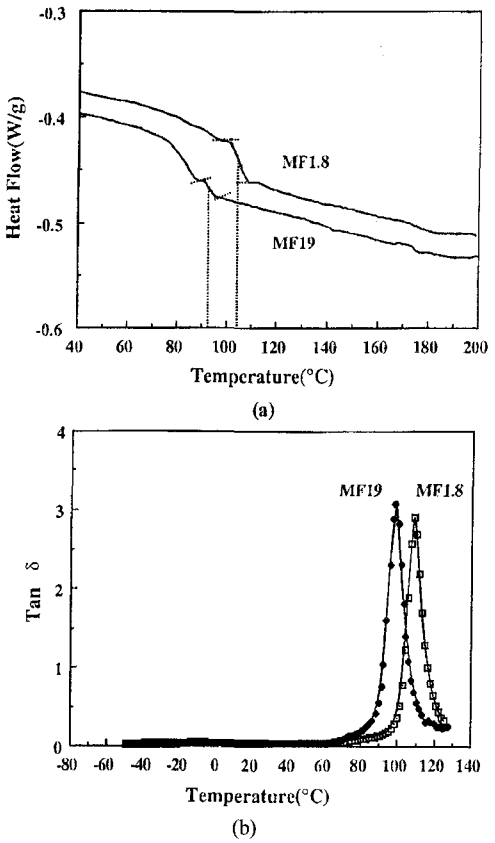


**Figure 1.** Measurement of glass transition temperature of PS by DSC (a) and DMTA (b) traces of PS samples.

those from DSC.

## 2. Tensile Properties of Polystyrene

The mechanical behavior of polymers is affected to a large extent by the changes in experimental conditions as well as the changes of molecular weight. The tensile stress-strain behavior of the two types of PS at different temperatures are depicted in Figure 2. A drastic change in the stress-strain curves appears at 83 ℃ for MF1.8. and 93 ℃ for MF1.8, respectively. This is the well-known brittle-ductile(B-D) transition and is observed about 10 ℃ below Tg of two PS. Below these temperatures, crazes form normal to the tensile direction beyond a critical stress (crazing stress) before fracture. The fracture stresses and strains increase with decreasing temperature since the volume of crazes increase with the development of craze yielding.[9] At low temperature, the molecules are frozen and the tensile strength is high. Thus, PS shows typical brittle properties. As the temperature increases, however, the chain mobility and relaxation of entanglement increase, and tensile stresses decrease. When the temperature reaches the B-D transition, PS is no longer brittle and shows a distinct yield/plastic deformation behavior. After yield point, the specimen exhibits necking and further cold drawing. Above this temperature, the specimen deforms uniformly without neck formation like rubbery materials. Instead of crazes, shear band formation at the surface of the specimen is observed in this process.

The strain rate and temperature dependence of the fracture and yield stresses of two types of PS are

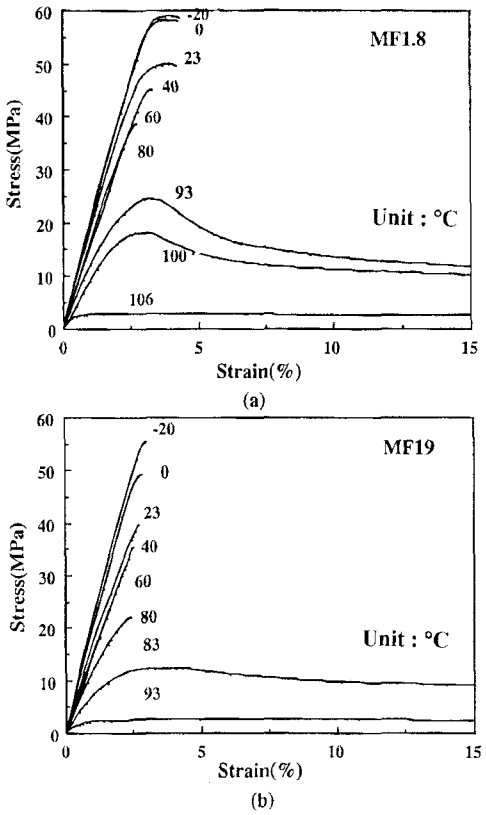


**Figure 2.** Stress-strain curves of (a) MF1.8 and (b) MF19 at a strain rate of 0.508 $min^{-1}$.

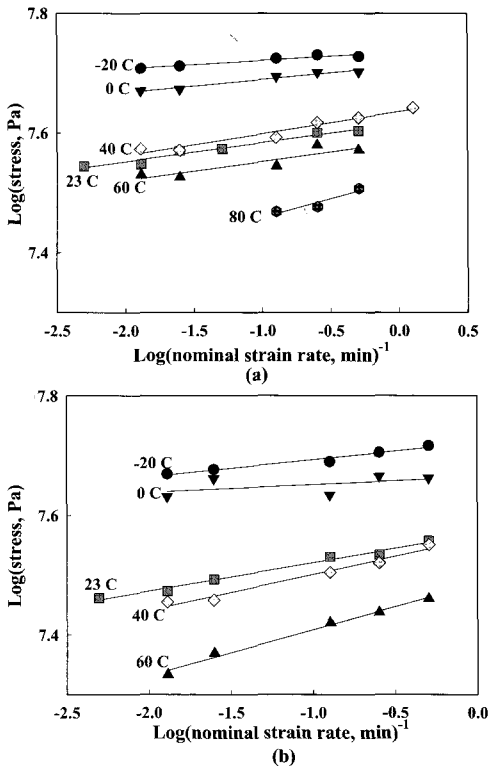


**Figure 3.** Tensile and yield stress at different temperatures and strain rates for (a) MF1.8 and (b) MF19.

shown in Figure 3. Both MF1.8 and MF19 exhibit two distinct transition regions in which the slopes of the log-log plots are changed at the temperature range -20 to 100 ℃. At these transition temperatures, the stress shows a substantial lowering. The yield process governs the B-D transition at higher temperatures between 80 and 100 ℃. The other transition at which the tensile stress exhibits much less temperature dependence than that at B-D transition temperature is observed around 23 ℃. At this temperature, the craze initiation stress as well as the fracture stress show an irregular temperature dependence. This result is depicted in Figure 4. Similar irregular temperature dependence of the craze initiation stress in PS has been observed by Haward et. al[10] and Matsushinge et. al.[11] The irregular temperature dependence might be related to the β-relaxation in PS. The DMTA result shows that the β-relaxation temperature of MF1.8 and MF19 are about 10 ℃ and 15 ℃, respectively. In Figure 5, the β-relaxation consists of double peaks covering a range from -20 ℃ to 40 ℃. Wunberlich and Bodily[12] detected the β-peak using a dynamic differential thermal analyzer (DDTA) as covering the range from -25 ℃ to 70 ℃ but centering around 27 ℃. Boyer[13] has suggested that the chain axis and β-relaxation is related to a crankshaft motion about the chain axis and β-relaxation temperature changes with experimental conditions.

In the brittle region, the fracture stresses decrease slowly with temperature and with increasing strain rate. Increase of fracture stress with strain rate and with decreasing temperature has already been observed in PS[14] and other polymeric materials.[15,16] As shown in Figure 6, however, the strain rate dependence of the fracture and yield stresses decrease at -20 ℃ compared to others at the temperature ranges of 0 ℃ to 100 ℃. The strain rate dependence of the fracture stresses increases with decreasing temperature from Tg and the fracture stresses become almost same at a certain temperature well below Tg. By adapting time-temperature superposition, a master curve for each

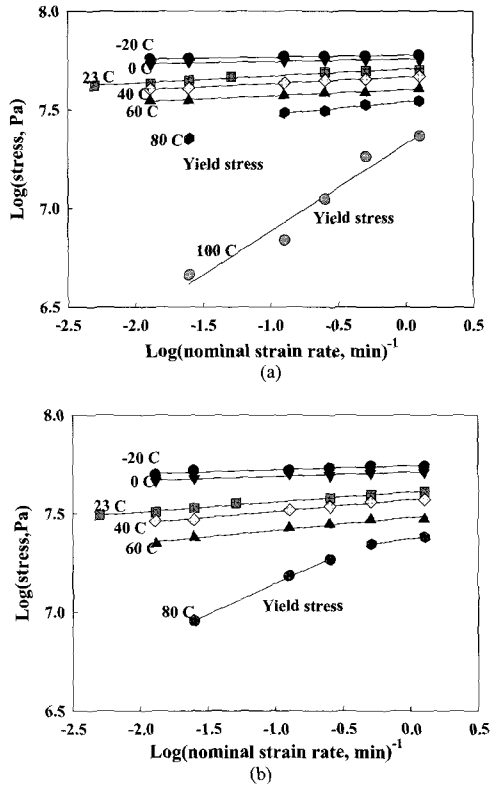


**Figure 4.** Crazing stress at different temperatures and strain rates for MF1.8 and (b) MF19.

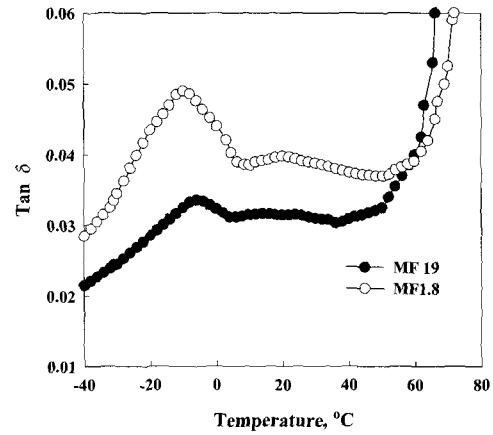


**Figure 5.** Measurement of β-relaxation temperature of PS on DMTA β-relaxation peaks of PS sample.

type of PS could be constructed. The master curves are shown in Figure 7. These curves show a plateau

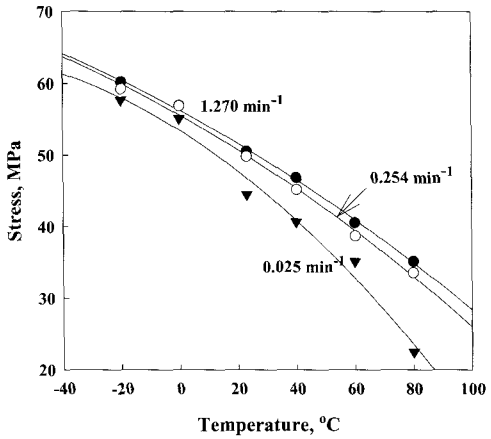


**Figure 6.** Tensile stress of MF1.8 at different strain rates and temperatures.

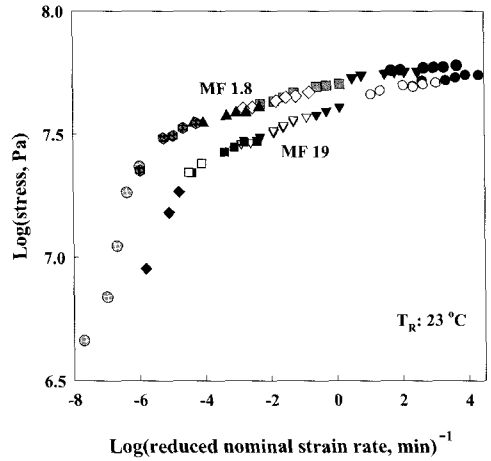


**Figure 7.** Master curves for MF1.8 and MF19 samples.

for the brittle tensile stress, and a transition and a flow region for the yield stress. The increase in tensile stress in the plateau region and the transition shift to lower strain rate for MF1.8 with higher molecular weight is attributed to increased degree of entanglements.

## Ⅳ. Crazing Behavior

### 1. Effect of Molecular Weight

For higher MW PS ($M_n$ = 125,000 g/mole), MF 1.8, the crazes are numerous, long, and very straight. Crazes of MF1.8 spread completely across the specimen at 23 ℃ during the entire range of strain rate before failure occurs (Figure 8(a)). This means that crazes of MF1.8 grew completely across the section of the specimen before significant crack growth occurred within the crazes. However, under the same test conditions, very short and fewer than those of MF1.8-crazes are formed in lower MW PS ($M_n$= 58,000 g/mole), MF19 (Figure 8(b)). Failure occurs in MF19 before the crazes have spread across the section of the specimen. For both MF1.8 and MF19, the crazes on the craze plane are parallel to each other without intersection. The difference of craze length and craze density between MF1.8 and MF19 is quantitatively described later.

As shown in Figure 2, the stress-strain curves of MF1.8 below 40 ℃ show the development of

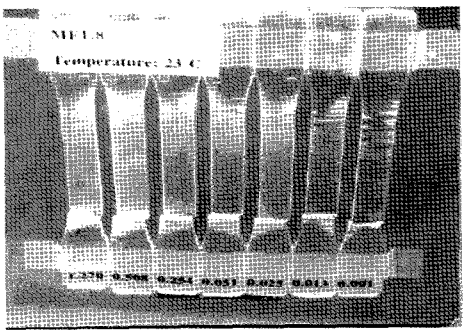

(a)

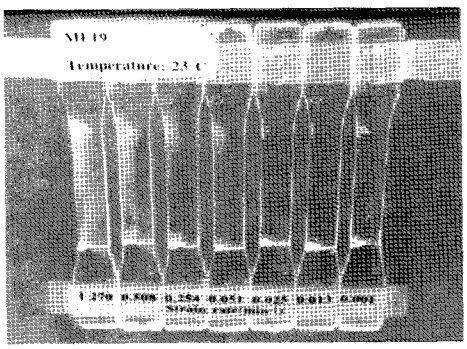

(b)

**Figure 8.** Comparison of crazing behavior at different strain rates for (a) MF1.8 and (b) MF19.

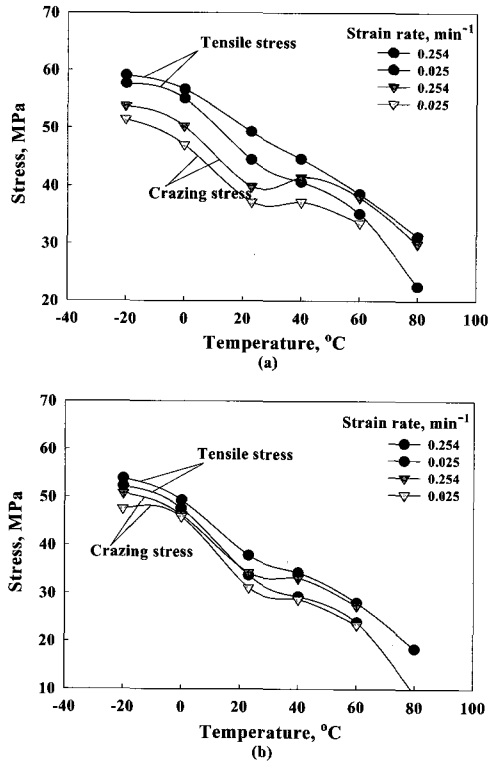


**Figure 9.** Tensile stress and crazing stress at different temperature and strain rate for MF1.8 and MF19.

characteristic craze yielding. However, in the case of MF19, the craze yielding occurs below 0 ℃, and the extent of craze yielding is much less than that of MF1.8. The time-temperature dependence of the crazing stress is illustrated in Figure 4. The crazing onset stresses decrease with strain rate and with increasing temperature similar to the behavior of the fracture stresses. The decrease of the onset crazing stresses with increasing temperature are more prominent for MF19 than MF1.8. Compared to the fracture stresses, it also can be seen that the onset crazing of stress does not fall so sharply at high temperature (Figure 9) as the fracture stresses. This result would be expected if crazing has to provide the nucleation surface energy for voids since this quantity would not be changed quickly with temperature. In this figure, the gap between the crazing stress and breaking stress of MF1.8 is much larger than that of MF19. Thus, the craze fibrils of MF1.8 have more time to grow than those of MF19. The difference of the craze texture between the two types of PS results from the fact that a critical MW for stabilizing craze fibrils is typically 2Mc[1,17] (the Mc of PS is around 35,000 g/mole). For MF19, crazes can only be formed in the higher molecular weight portion than 70,000 g/mole since MF19 shows very broad molecular weight distribution. Thus, craze structure of MF19 is unstable and jagged. This indicates that chain entanglement is important in stabilizing fibrils. Only the ability to strain-harden upon drawing confers stability on the craze, which rules out crazing in low molecular weight polymers.

## 2. Effect of Temperature

As the testing temperature decreases, the number of crazes increases and the texture of crazes become long for MF1.8 (Figure 10). As shown in Figure 9, the breaking stress and the difference between the crazing onset stress and the breaking stress increase slightly with decreasing temperature. Thus, the crazes of both MF1.8 and MF19 have more time to grow to the direction of thickness and length with decreasing temperature. The temperature dependence of crazing behavior is associated with the stability of entanglement-craze fibril stability.[4]

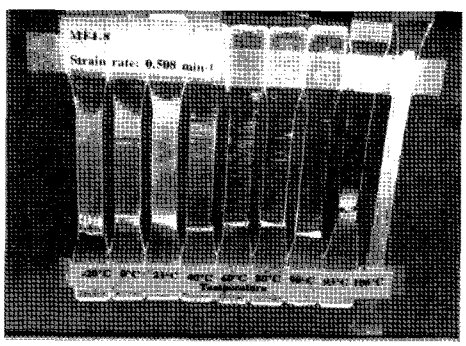

**Figure 10.** Crazing behavior of MF1.8 at different temperature.

## 3. Effect of Strain Rate

As strain rate increases, the number of crazes increases and the structure of crazes become long for both MF1.8 and MF19 since increase in strain rate results in stabilizing craze fibrils. As shown in Figure 9, the crazing onset stress and the gap between the crazing onset and the fracture increase slightly with increasing strain rate for both MF1.8 and MF19. As the result, the volume of crazes in a specimen increases with strain rate. The strain rate dependence of crazing behavior is equivalent to some decrease in temperature.

## 4. Craze Density and Length

In tensile testing, an extensive growth of crazes across the gauge length of the specimen occurs beyond a critical level of stress. As shown in Figure 11, above the critical stress the average length of the crazes and the standard deviation of the average craze length increase, and the number of crazes also increase before fracturing. The craze density changes exponentially (Figure 11a) to the applied stress. This means that at the initial stage, the nuclei of crazes slowly formed in the area which nucleation surface energy forms into voids. However, once a certain number of crazes are formed through increasing stress, the area between these growing craze tips would be highly stress-concentrated. This higher stress concentration would speed up the nucleation of crazes more and more. This result suggests that the craze growth and the onset of new crazes occur at same time. When the fracture occurs, the number of crazes is about 700 for MF1.8 and about 400 for MF19. The average length of crazes is about 0.15 cm for MF19 and 0.4 cm for MF1.8. The above values for MF1.8 were obtained from the regression of the plot. The craze density of MF1.8 at the fracture site could not be measured with a cathetometer since the crazes were too numerous to count.

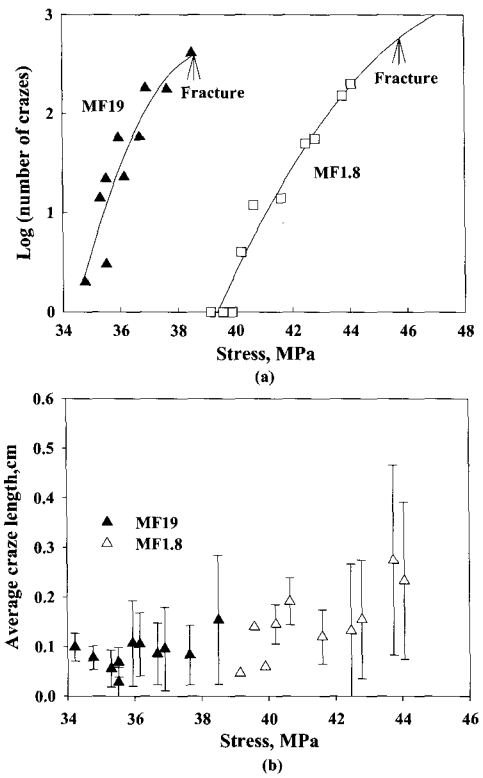


**Figure 11.** The change of (a) the number and (b) average length of crazes at 23 ℃ and a strain rate of 0.127 $min^{-1}$ during tensile test.

## 5. Craze Structure

The material inside the craze is strongly plastically deformed normal to the craze plane. The craze fibrils in PS consists of plastically oriented polymer and are parallel to each other. The craze fibrils in the bulk specimen observed by AFM (Figure 12) have coarser structure than the craze in reference.[18] From figure 12, the craze thickness and the fibril diameter of MF1.8 at 40 ℃ and a strain rate of 0.013 $min^{-1}$ is about 0.4 $\mu$m and 110 nm, respectively. According to Kambour[3] and Michler,[19] craze fibril diameters are 0.6 to approximately 30 nm and craze thickness are 1 to 10 $\mu$m in most crazes of PS formed far below Tg. Compared to these results, it can be concluded that some relaxation of the crazes in the bulk PS specimen occurs after the tensile stress was removed.

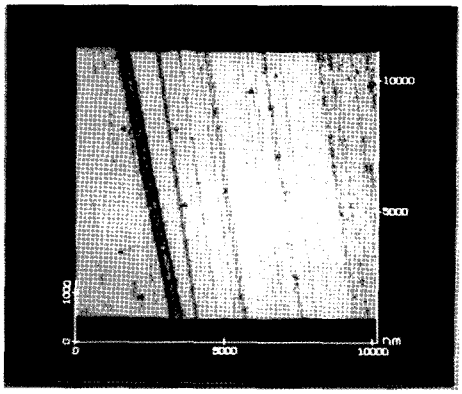


(a)

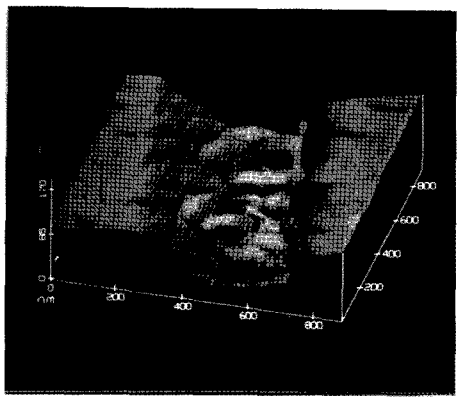


(b)

**Figure 12.** Atomic force micrograph of craze fibrils in MF1.8 at 40 ℃ and a strain rate of 0.013 $min^{-1}$ ; (a) top view of microtomed craze, (b) healed craze fibrils.

Since cracks result from a breakdown of the fibril structure within a craze, the craze structure is highly related to the fracture process and fracture surfaces have a lot of interesting features. The typical fracture surfaces of MF 1.8 and MF 19 at different temperatures and strain rates are shown in Figure 13. There is a sharp boundary between the pre-crazed fracture surface (mirror region-relatively smooth and even surface-dark area) and the bulk fracture surface (rough surface-bright area) in Figure 13(c). It can be stated from these optical micrographs that the textures of the fracture surfaces changed with such variables as MW, temperature, and strain rate. As temperature decreases, strain rate

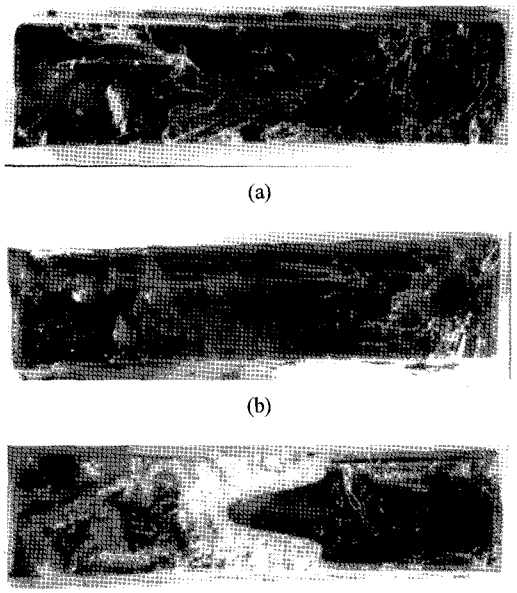

(a)

(b)

(c)

**Figure 13.** Optical micrographs of MF1.8 at (a) -20℃, (b) 23℃, (c) 60℃ and a strain rate of 0.254 $min^{-1}$. (x8).

and MW increase, the pre-crazed area on the fracture surface increases. Also the texture of the pre-crazed fracture surface becomes rougher by changing these variables. This indicates that a lot of craze planes are involved in a crack path-before fracturing occurs, the distance between craze planes decreases. Thus, it is suggested that the craze growth to the length direction would be enhanced, and the craze density increases with changing the variables such as temperature decreases, strain rate increases, and MW increases. It is also noticeable that the parabolic shape of a craze tip is blunted with increasing temperature and with decreasing MW. This indicates that the craze growth rate changes with different variables since a sharp craze tip advances faster than a blunt craze tip. From these optical micrographs, the region of crack initiation can easily be distinguished from the rest regions because the crack initiation region has a familiar concentric shape.

## V. Conclusions

The tensile stress and yield stress of polystyrene increased with molecular weight, strain rate, and decreasing temperature. The ultimate elongation showed the same behavior at the temperatures below the brittle-ductile transition due to the development of craze yielding. Polystyrene exhibited two distinct regions showing the irregular temperature dependence of tensile stress; the $\beta$-transition and the brittle-ductile transition. The temperature dependence of tensile stress at the $\beta$-transition temperature was much less than that at the brittle ductile transition temperature. Crazes formed in the brittle fracture region. At low temperature, in case of high molecular weight sample, crazes were well developed in the entire area of specimen, and spread completely across the specimen. However, the average length and the number of crazes decreased with molecular weight and increasing temperature. The crazing stress increased with molecular weight, strain rate, and with decreasing temperature. However, the dependence was small compared to the tensile stress. The gap between crazing stress and tensile stress which reflected time for craze formation and growth increased with molecular weight, strain rate, and with decreasing temperature. During tensile testing, the craze density changed exponentially. At the initial stage, crazes formed slowly. Once a certain number of craze formed, however, the craze density increased rapidly. Craze nucleation and growth occurred at the same time. There was a sharp boundary between the pre-crazed fracture area and the bulk fracture area. The pre-craze fracture area increased with molecular weight, strain rate, and with decreasing temperature.

## References


1. R. P. Kambour, "A Review of Crazing and Fracture in Thermoplastics", *Macromol. Rev.*, **7**, 1(1973).
2. E. J. Kramer, "Microscopic and Molecular Fundamentals of Crazing" in "Advances in polymer Science", H. H. Kausch Ed., Vol.52/53, Springer-Verlage, Berlin (1983).
3. R. P. Kambour, Crazing. in "Encyclopedia of Polymer Science and Engineering" J. I. Krischwitz Ed., 2nd Ed., Vol.4, John Wiley & Sons, N. Y. (1985)
4. E. J. Kramer and L. L. Berger, "Fundamental Processes of Craze Growth and Fracture. in "Advances in Polymer Science", H. H. Kausch Ed., Vol.91/92, Springer-Verlage, Berlin (1990).
5. J. Murry and D. Hull, "Nucleation and Propagation of Cracks in Polystyrene", *Polymer*, **10**, 451 (1969).
6. J. Murry and D. Hull, "Fracture Surface of Polystyrene: Mackerel Pattern", *J. Polym. Sci.*, **8**, 583 (1970).
7. B. D. Lauterwasser and E. J. Kramer, "Microscopic Mechanisms and Mechanics of Craze Growth and Fracture", *Phil. Mag.*, **39(4)**, 469 (1979).
8. J. Hoare and D. Hull, "The Effect of Temperature on the Deformation and Fracture of Polystyrene", *J. Mater. Sci.*, **10**, 1861 (1975).
9. J. Hoare and D. Hull, "Craze yielding and Stress-Strain Characteristics of Crazes in Polystyrene", *Phil. Mag.*, **26**, 443 (1972).
10. R. N. Haward. B. M. Murphy, and E. F. T. White, "Relationship between Compressive Yield and Tensile Behavior in Glassy Thermoplastics", *J. Polym. Sci.*, **A-2**, **9**, 801 (1971).
11. K. Matsushige, S. V. Radcliff, and E. Baer, "Relationship Between Compressive Yield and Tensile Behavior in Glassy Thermoplastics", *J. Appli. Polym. Sci.*, **20**, 1853 (1976).
12. B. Wunderlich and D. M. Bodily, "Dynamic Differential Thermal Analysis of the Glass Transition Interval", *J. Polym. Sci., C*, **6**, 137 (1964).
13. R. F. Boyer, "Dependence of Mechanical Properties on Molecular Motion in Polymers", *Polym. Eng. Sci.*, **8(3)**, 161 (1968).
14. J. R. Martin, J. F. Johnson, and A. R. Cooper, "Mechanical Properties of Polymers: The Influence of Molecular Weight and Molecular Weight Distribution", *J. Macromol. Sci.-Revs. Macrmol. Chem.*, **C8**, 57 (1972).
15. O. Inhai, "Delayed Yielding of Epoxy Resin Under Tension, Compression, and Flexure. I.

Behavior Under Constant Strain Rate", *J. Polym. Sci.*, **11**, 963 (1967).
16. A. E. Moehlenpah, O. inhai, and A. T. Dibenedetto, "The Effect of Time and Temperature on the Mechanical Behavior of a "Plasticized" Epoxy Resin Under Different Loading Modes", *J. Appl. Polym. Sci.*, **13**, 1231(1969).
17. J. E. Fellers and B. F. Kee, "Crarzing Studies of Polystyrene. I. A. New Phenomenological Observation", *J. Appli. Polym. Sci.*, **18**, 2355(1974).
18. N. Brown and X. Wang, "Direct Measurements of the Strain on the Boundary of Crazes in Polyethylene. *Polymer"*, **29**, 463 (1988).
19. G. H. Michler, "Correlation Between Craze Formation and Mechanical Behavior of Amorphous Polymers", *J. Mater. Sci.*, **25**, 2321 (1990).